Electronic structure of impurity (oxygen)–stacking-fault complex in nickel

Wang Chong-yu
China Center of Advanced Science and Technology (World Laboratory), P.O. Box 8730, Beijing and Central Iron and Steel Research Institute, Beijing, People's Republic of China

Liu Sen-ying and Han Lin-guang
Central Iron and Steel Research Institute, Beijing, People's Republic of China
(Received 2 August 1988; revised manuscript received 8 August 1989)

Based on related experiments, in this paper a model is presented to study the electronic structure of an impurity–stacking-fault complex. Using the tight-binding Hamiltonian and recursion method, we have calculated the electronic structure of systems containing an impurity–stacking-fault complex. Based on the calculation of the structural energy, the relation between impurity and stacking-fault energy was given. It found that impurity oxygen increased the stacking-fault energy of the Ni system, whereas impurity Fe decreased it markedly, which has been proved by our electron-microscope experiments. Calculations of the partial-wave integral local density of states for atoms give information on the local charge transfer and hybridized orbital.

I. INTRODUCTION

Our experiments[1] discovered that trace-element oxygen in Ni-Fe–based alloys affected the type of the deformation texture, primary recrystallization texture, and recrystallization process, and related to properties of the alloy.

In order to investigate the mechanism of action of trace-element oxygen existing in a dilute alloy, we have presented a model of an impurity (oxygen)–stacking-fault complex. In this paper we calculate the electronic structure of a light impurity (oxygen)–stacking-fault complex by a recursion method combined with a tight-binding Hamiltonian. The local density of states (LDOS) is obtained. From the LDOS, the structural energy and charge transfers of the impurity and its neighbors can be gained. Based on the calculation of the electronic structure, we get the stacking-fault energy, the attached surface energy on the stacking-fault plane, and the effect of stacking faults on the motion of the dislocation. The results show that the effect of the electronic structure of the impurity (oxygen)–stacking-fault complex on the stacking-fault energy and the motion of the dislocation is very important. To ascertain the effect of the alloying element Fe in a Ni-Fe–based alloy on the stacking-fault energy, we also calculated the electronic structure of the Fe–stacking-fault complex, which shows that Fe on the stacking-fault plane decreased the stacking-fault energy markedly.

On the other hand, our experimental electron-microscope results on stacking faults in Ni and Ni-Fe–based alloys and of x-ray diffraction on the stacking-fault energy of the Ni system has shown that in the Ni-Fe–based alloy specimen without oxygen, the typical stacking fault can be observed, and its width may reach 4000 Å, but when the oxygen content in the alloy increases to the order of 10^{-4} (corresponding to 0.01 wt. %), it is very difficult to find the stacking fault in the specimen. So our basic physical idea and calculation results of the electronic structure have been proved.

II. PHYSICAL MODEL

Our basic physical idea is that atomic defects (such as an impurity, alloying element, etc.) combined with structural defects (such as a stacking fault, vacancy, dislocation, etc.) form a local unit in a solid, which affects the material properties by electronic effects and phonon excitation.

For oxygen contents in the alloy of the order of 10^{-4} (corresponding to 0.01 wt. %), the alloy can be considered to be a dilute alloy. Ni or Ni-Fe–based alloys are of the fcc structure with an arrangement of $\cdots ABCABC\cdots$ along the $\langle 111\rangle$ direction. The intrinsic stacking fault[2,3] with one layer of C being extracted corresponds to a hcp structure of the mosaic block being inserted in the fcc structure, which is shown in Fig. 1. In this paper we let the impurity oxygen atom lie in the hole of the octahedron in the stacking-fault region of the Ni system. From it we set up a single-impurity model of

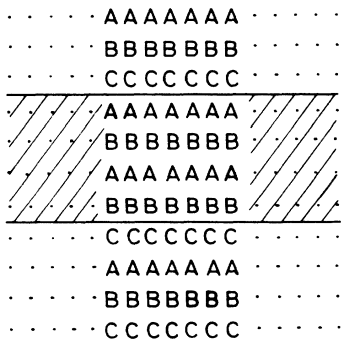

FIG. 1. The stacking-fault structure in a fcc crystal.

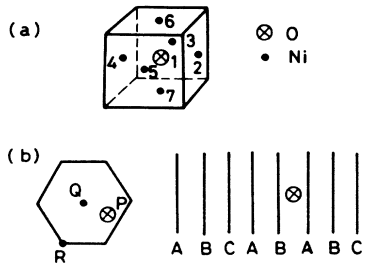

FIG. 2. (a) The NaCl-type structure of oxygen and its first neighbors. (b) The crystal sites of the interstitial oxygen in the stacking-fault region and its neighbors: site p, the position where oxygen locates; site Q, the impurity's first neighbor; site R, the impurity's second neighbor.

a light impurity (oxygen)–stacking-fault complex, as shown in Fig. 2. Considering the local effect of the impurity-defect complex, this paper uses a tight-binding Hamiltonian.

To investigate the effect of a substituent alloying element Fe on the stacking-fault energy, and considering the content of the alloying element Fe above 10 wt. % having a chance to combine with the stacking fault, we present a local model in Fig. 3.

III. CALCULATION METHOD AND PARAMETER CHOICES

To deal with the solid problem containing disordered distributive impurities and structural defects, it is necessary to set up a new physical idea and theoretical method[4] which are different from traditional band theory. When the electrons interact strongly with the atoms, the characteristic of the electron is mainly determined by each atom's neighbors. The local density of states can describe the feature. In this paper we used the recursion method[5] to give the local density of states for the model system. The effect of the recursion method is to transform a quantum-mechanics problem into a chain

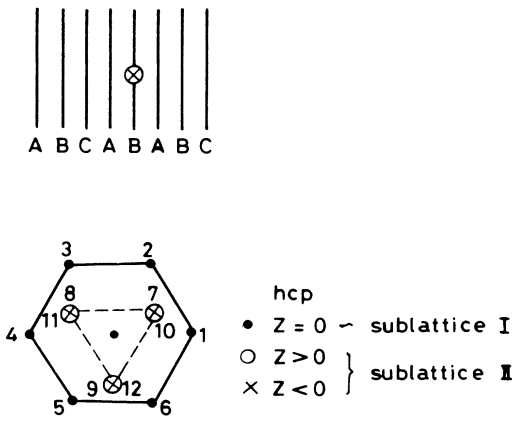

FIG. 3. The projection on the plane $z=0$ of the first neighbors of the impurity Fe in hcp structure, which is a model describing Fe-Ni–based alloys.

model represented by a set of orthonormalized basis sets $\{u_n\}$ and real parameter sets $\{a_n\}$ and $\{b_n\}$. The set $\{u_n\}$ satisfies the recurrence relation

$$H|u_n\rangle = a_n|u_n\rangle + b_{n+1}|u_{n+1}\rangle + b_n|u_{n-1}\rangle \ . \tag{1}$$

In Eq. (1), H is the tight-binding (TB) Hamiltonian, the diagonal elements are expressed by the atomic potential, and the off-diagonal elements are given by the Slater-Koster integral.[6] In this paper, we are interested in the relative effects of the impurity–stacking-fault complex on the periodic crystal. This paper used the parameter-fitting potential,[7] which may reflect the relative changes caused by the impurity-defect complex.

For the TB Hamiltonian and the linear combination of atomic orbitals (LCAO) method, at the first approximation, this paper took the atomiclike orbital $|\varphi_\alpha\rangle$ as the local orthonormal basis set which meets the general needs of the recursion method. In the recurrence relation, referred to an empirical rule, the truncation of the basis set $\{u_n\}$ was taken as $n=2N_c$, N_c is the least number of steps of first-neighboring atoms from the center of the cluster to the boundary. There exists a unitary transformation between the basis set $\{u_n\}$ and the local atomic orbital $|\varphi_\alpha\rangle$.

From the recurrence relation it is proved that the Hamiltonian matrix H can be tridiagonalized in the representation of an orthonormalized set $\{u_n\}$, i.e.,

$$H^{\text{tri}} = \begin{bmatrix} a_0 & b_1 & & \\ b_1 & a_1 & b_2 & \\ & b_2 & a_2 & \ddots \\ & & \ddots & \ddots \end{bmatrix} . \tag{2}$$

The Green operator is

$$G(E) = (E - H^{\text{tri}})^{-1} \ . \tag{3}$$

It can be proved from Eq. (3) that the diagonal elements of the local Green's function

$$G_{\alpha l,\alpha l} = \langle \alpha, l|(E + i0 - H^{\text{tri}})^{-1}|\alpha, l\rangle \tag{4}$$

may be expressed as a continued fraction. Based on the definition of the LDOS,

$$n_{\alpha l}(E) = \sum_n |a_{n,\alpha l}|^2 \delta(E - E_n) \tag{5}$$

in the linear combination of orbitals representation, the LDOS for site l and orbital α can be written as follows:

$$n_{\alpha l}(E) = -\pi^{-1}\text{Im}[\langle \alpha l|(E + i0 - H^{\text{tri}})^{-1}|\alpha l\rangle] \tag{6}$$

$$= -\pi^{-1}\text{Im}\cfrac{1}{E - a_0 - \cfrac{b_1^2}{E - a_1 - b_2^2/E - a_2 \cdots}} \tag{7}$$

thus, it is easy to carry out numerical calculations.

It is easy to see that the recursion method is an effective implement to obtain the spectrum of any operator and can be used to study the electronic structure of ordered or disordered systems. This paper selects the long-chain model and uses a special method[5,8] to smooth

the discrete spectrum to give the smoothed LDOS.

In this paper we used the Harrison parameter[7] to give the transition integral for our model system. In the LCAO representation and with the neighboring approximation, the tight-binding Hamiltonian is simplified to a sparse matrix including many zero elements. The corresponding Hamiltonian matrix element can be expressed as a Slater-Koster integral

$$E_{\mathrm{SK}} = \sum_m f(\mathbf{V}_{AB}) V_{ll'm} \ . \tag{8}$$

In Eq. (8), $f(\mathbf{V}_{AB})$ is a function of the cosine direction of the direction of the vector $\mathbf{R}_A - \mathbf{R}_B$, pointing from one atom to the other. $V_{ll'm}$ is the transition integral,

$$V_{ll'm} = \langle lm|H|l'm \rangle \ , \tag{9}$$

where l and l' are the angular quantum numbers and m is the magnetic quantum number.

The system for numerical calculation includes 3122 particles, that is to say the whole background has 3122 atoms. In this paper TB Hamiltonians are only involved in the interaction between the first-neighboring atoms, that is to say, the transition integral $v_{ll'm}$ only calculates the orbital interaction between the first-neighboring atoms. Based on the recurrence relation, the continued fractions $\{a_n\}$ and $\{b_n\}$ can be given. From it, the DOS can be obtained. The recurrence relation expresses the "recursion" effects going outward from the center.[4] Hence, from the changes of the DOS of different neighboring atoms of the central atom, the effects of the central atom on the different neighboring atoms can be seen. The electron configurations of the atoms are O $2s^2 2p^4$, Ni $3d^8 4s^2$, and Fe $3d^6 4s^2$.

IV. CALCULATION RESULTS OF ELECTRONIC STRUCTURE FOR A MODEL SYSTEM AND RELATED EXPERIMENTS

A. Local density of states

To describe the "characteristics of a spectrum" of a model system, we have calculated the local density of states, which is shown in Figs. 4–7. Figure 4 gave the superposition of the DOS curves for Ni(6) and Ni(6)-O small clusters. The background for both of these two small clusters is 3122 atoms (for the system containing the oxygen the background has 3123 atoms). In Fig. 4, curve 1 and curve 3 show that the stacking fault makes some changes of the DOS of the cluster. The feature of the DOS of the Ni(6) cluster containing the stacking fault (curve 3) is splitting of the degenerate state of d electrons (from $\{a_n\}$ and $\{b_n\}$, this change also can be seen obviously); curves 2 and 4 give the change of the DOS of the systems containing oxygen and containing an oxygen–stacking-fault complex relative to the system without oxygen, respectively. In Fig. 5, the relative change between curves 1 and 2 gives the detail of the DOS peak and the effect of the stacking fault on it (curve 2 is of stacking-fault Ni); curve 3 is the DOS of the first-neighboring Ni of central oxygen. From it we can see the

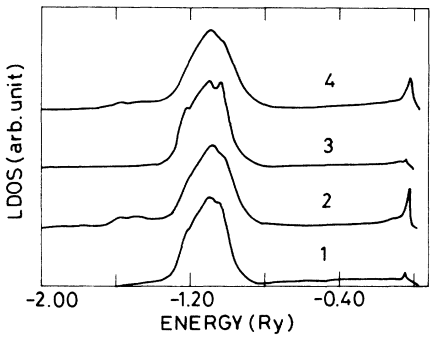

FIG. 4. LDOS of the clusters for various systems. Curves 1 and 3 stand for the LDOS of the cluster Ni(6) in pure Ni systems with and without the stacking fault, respectively. Curves 2 and 4 stand for the LDOS of the cluster Ni(6)0 in Ni systems with the impurity oxygen and with the impurity (oxygen)–stacking-fault complex, respectively.

feature of the DOS of Ni when an impurity–stacking-fault complex exists. It is different from curve 2 when there only exists a stacking fault. Curve 4 is the DOS of the second-neighboring Ni of the central oxygen (this atom is on the stacking-fault plane), which shows that the effect of oxygen on it is weakened and the effect of the stacking fault on it is obvious. Curve 5 is the DOS of the third-neighboring Ni. This Ni atom is not on the stacking-fault plane, therefore, the effect of the stacking fault on it is partly weakened. For the DOS of the fourth-neighboring Ni (curve 6), it appears that the feature of the stacking fault is again due to this Ni atom on the stacking-fault plane. The more distant Ni atoms

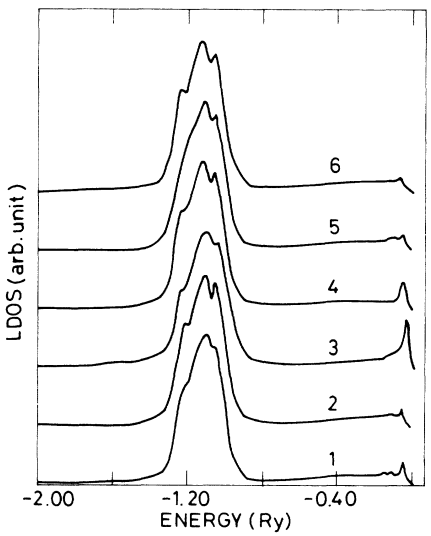

FIG. 5. LDOS of atoms for various systems. Curves 1 and 2 stand for the LDOS of the center Ni atom in Ni systems with and without the stacking fault, respectively. Curves 3–6 stand for the LDOS of the impurity oxygen's first- through fourth-neighbor Ni in a Ni system with the impurity (oxygen)–stacking-fault complex, respectively.

are not on the stacking-fault plane, so the effects of the stacking fault on them disappear gradually.

Figure 6 gave the LDOS of the first-neighboring Ni of the central oxygen in the system containing an impurity–stacking-fault complex. The result reflects the details of the triply degenerate d state [$d_1(xy)$, $d_2(yz)$, and $d_3(zx)$] and doubly degenerate d state [$d_4(x^2-y^2)$ and $d_5(3z^2-r^2)$], and the local property of the d state.

Figure 7 is the LDOS of impurity oxygen in the system containing an impurity–stacking-fault complex; it is easy to see that the s and p electrons are the extended state.

Comparing the LDOS of Ni containing the stacking fault with that of Ni without it, one can see that the conspicuous splitting of the peak of d electrons in the LDOS of Ni with the stacking fault shows the effect of the stacking fault on the doubly degenerate (E_g) and the triply degenerate (T_{2g}) symmetries. (The change in the data of real parameter sets $\{a_n\}$ and $\{b_n\}$ reflects this feature.)

B. Trace-element oxygen, alloying element Fe, and stacking-fault energy

1. *Stacking-fault energy for single-element Ni*

Structural energy at site l is defined as

$$E_l = \int_{-\infty}^{E_F} E \sum_{\alpha} n_{\alpha l}(E)dE \ , \tag{10}$$

where E_l is a characteristic parameter in the local description. The Fermi level of the system is determined by

$$N = \int_{-\infty}^{E_F} \sum_{\alpha} \sum_{l} n_{\alpha l}(E)dE \ , \tag{11}$$

where N is the total number of valence-electron occupation states in the system.

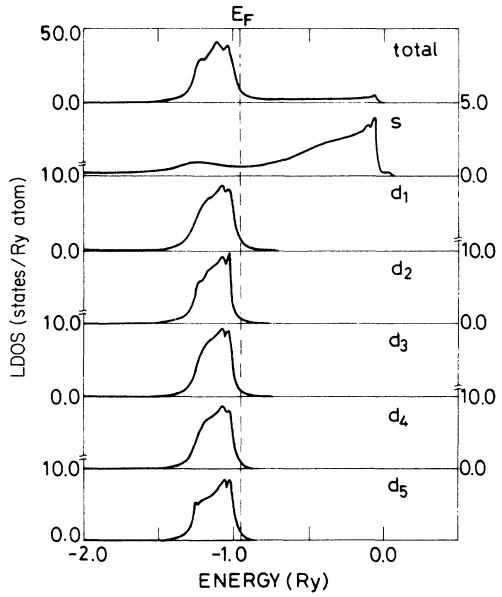

FIG. 6. LDOS and partial-wave LDOS of the impurity oxygen's first-neighbor Ni in a Ni system with the impurity (oxygen)–stacking-fault complex.

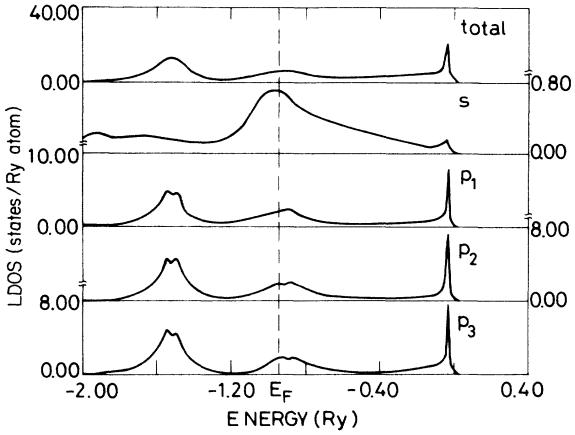

FIG. 7. LDOS and partial-wave LDOS of impurity oxygen in a Ni system with the impurity (oxygen)–stacking-fault complex.

The structural energy of the system is as follows:

$$U = \sum_{l} E_l \ . \tag{12}$$

It contains almost all of the interesting structure-dependent parts of the energy.[4] In a close-packed solid, we used the Wigner-Seitz approximation and considered the order of the difference between $U_{\text{Hartree}}^{\text{intra-atom}}$ and $U_{\text{ex}}^{\text{intra-atom}}$ to be considerably smaller than that of U; therefore, we can use $U=\sum_l U_l$ to approximately express the total energy, which is used to study the relative change of the energy of the system caused by the structural defect. Because the stacking fault causes a change in the energy of the system, it can be expressed as follows:

$$\Delta U = U_1 - U_0 \ , \tag{13}$$

where U_1 and U_0 are the energies of the systems with and without the stacking fault, respectively.

We define stacking-fault energy as

$$E_{\text{sf}} \equiv \frac{\Delta U}{\Delta S} \ . \tag{14}$$

Equation (14) expresses the energy required to form a stacking fault per unit area.

From calculation of the structural energy of the Ni system with and without the stacking fault, we have given a contribution of electrons to the stacking-fault energy: $(E_{\text{SF}}^{\text{Ni}})_{\text{el}}=152.8$ erg/cm^2, which is very close to the result of Ref. 9 [contribution of the phonon excitation to the stacking-fault energy is very small, $(E_{\text{SF}}^{\text{Ni}})_{\text{ph}}=0.193$ erg/cm^2 (Ref. 3)].

The calculating model used to calculate the stacking-fault energy is shown in Fig. 8. The calculated sites are covered from the center layer to the fourth misfit layer, meanwhile, we measured the stacking-fault energy of single-element Ni by the x-ray-diffraction method, which is $E_{\text{SF}}^{\text{Ni}}=202$ erg/cm^2.

Based on the equilibrium condition in which the sur-

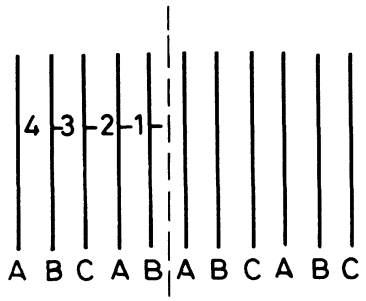

FIG. 8. The calculation model of the stacking-fault energy.

face tension on the stacking-fault plane and the repulsive force between the partial dislocations were established, the equilibrium width of the extended dislocation can be given,[2]

$$D=\frac{\mu b_1^2}{8\pi E_{\mathrm{SF}}}\frac{2-\nu}{1-\nu}\left[1-\frac{2\nu}{2-\nu}\cos 2\psi\right] . \tag{15}$$

In the formula, μ is the elastic modulus, ν is the Poisson ratio, ψ is the angle between Burger's vector of the perfect dislocation and the line of the dislocation. From Eq. (15), when $F_{\mathrm{SF}}^{\mathrm{Ni}}=150$ erg/cm^2, it gives $D=8$ Å.

On the basis of our calculation, we can predict that in single-element Ni, the stacking fault will not be observed. In fact only some perfect dislocations can be observed. The samples used to examine a transmission electron microscope were prepared by employing a double-jet polishing and ion thinning. A thickness of under 2000 Å was reached in general. Magnification was given in the figure captions. Our electron-microscope experiment, which is shown in Fig. 9, indicates that this is true.

2. *Stacking-fault energy of the Ni-O system with a stacking fault*

According to

$$E_{\mathrm{SF}}^{\mathrm{Ni\text{-}O}}=\frac{\Delta U}{\Delta S} , \tag{16}$$

we calculated the stacking-fault energy of the Ni-O system with a stacking fault, which atomic structure was shown in Fig. 2, and gave $E_{\mathrm{SF}}^{\mathrm{Ni\text{-}O}}=203.5$ erg/cm^2. From $E_{\mathrm{SF}}^{\mathrm{Ni}}=152.8$ erg/cm^2, it is easy to see that the attached surface energy due to oxygen on the stacking-fault plane is $E_{\mathrm{att}}=50.9$ erg/cm^2. Obviously, in the Ni-O system, the stacking fault cannot be observed, which is also proved by our electron-microscope experiment. The electron-microscope image of the Ni system with oxygen ($>10^{-4}$ order, that is to say, >0.01 wt. %) is shown in Fig. 10, which is similar in shape to that of Ni without oxygen. We have not observed the stacking fault but we have seen a lot of networks of dislocation.

For the system containing the interstitial impurity –stacking-fault complex, the stacking-fault energy is expressed as follows:

$$\frac{\Delta U}{\Delta S}=\left[\sum_l \frac{E_l}{N}-\sum_l \frac{E_l^0}{N_0}\right]\Big/\Delta S , \tag{17}$$

where $N=N_0+n$, N_0 is the total number of the atoms in matrix, n the number of impurity atoms, and E_l the structural energy at site l in a Ni system with oxygen. E_l^0 stands for the structural energy in a matrix without impurity oxygen. $\sum_l$ covers the area of the impurity–stacking-fault complex. In our calculation, from the first-nearest to fourth-nearest neighbors of the impurity has been considered.

3. *Stacking-fault energy for a Ni-Fe–based alloy with a stacking fault*

For a Ni-Fe–based alloy, we have taken Fig. 3 as our single-impurity model. According to Eq. (16), the stacking-fault energy of the substitutent Fe-Ni–based alloy with a stacking fault has been given as follows: $E_{\mathrm{SF}}^{\mathrm{Ni\text{-}Fe}}=60$ erg/cm^2. Obviously, Fe makes the stacking-fault energy of the Ni system decrease markedly, which is opposite to the effect of impurity oxygen on it.

In the specimen of a Ni-Fe–based alloy used in the electron microscope Fe content reaches above 10 wt. %,

FIG. 9. The image of an electron microscope (magnification: 1.35×10^5) for the specimen of a Ni alloy without oxygen.

FIG. 10. Electron-microscope image (magnification: 1.35×10^5) for the specimen of the Ni alloy with oxygen.

so the effect of Fe on the stacking-fault energy can be larger than the effect of a single impurity Fe on it; thus, it predicted that in a Ni-Fe–based alloy without oxygen, the stacking-fault energy is very low. The stacking fault can be observed, which is confirmed by our electron-microscope experiment. The image of the stacking fault in a Ni-Fe–based alloy without oxygen is shown Fig. 11, its width reaches $D=3800$ Å. Relative electron-microscope research of the stacking fault for various alloys[9–12] also gave the similar electronic picture. In this kind of Ni-Fe–based alloy without oxygen, the frequency of appearance of the field reaches above 40%, that is to say, for 100 fields there are more than 40 fields in which the stacking fault can be observed. According to analyses of the electron diffraction image of the stacking fault, the direction along the width of the stacking fault is $\langle 110 \rangle$.

Meanwhile, we have also done the observation with an electron microscope for a series of Ni-Fe–based alloys with oxygen (>0.01 wt. %); the typical diffraction contrast image is shown in Fig. 12. The result shows that there are a lot of networks of dislocation. The corresponding image of the stacking fault is shown in Fig. 13, the frequency of the appearance of the field of the stacking fault is under 1%, which shows that the oxygen in the system markedly decreases the frequency of appearance of the field of the stacking fault.

C. Transfer of local electronic charge

Based on the following expressions, we discussed the local charge transfer in detail. The integral density of states at site l is

$$N_l=\int_{-\infty}^{E_F}\sum_{\alpha} n_{\alpha l}(E)dE \ . \tag{18}$$

Partial-wave integral density of states of the α orbital at site l is

FIG. 11. The image of the stacking fault (magnification: 4.8×10^4) for the specimen of a Ni-Fe–based alloy without oxygen.

FIG. 12. The typical diffraction contrast image (magnification: 2.8×10^4) for the specimen of a Ni-Fe–based alloy with oxygen.

$$N_{\alpha l}=\int_{-\infty}^{E_F} n_{\alpha l}(E)dE \ . \tag{19}$$

Valence-electron occupancy at site l is

$$Q_l=2N_l \ . \tag{20}$$

Valence-electron occupancy of the α orbital at site l is

$$Q_{\alpha l}=2N_{\alpha l} \ . \tag{21}$$

The transfer of charge at site l is as follows:

$$\Delta Q_l=2N_l-Q_l^v \ . \tag{22}$$

The transfer of charge of the α orbital at site l is

$$\Delta Q_{\alpha l}=2N_{\alpha l}-Q_{\alpha l}^v \ , \tag{23}$$

FIG. 13. The image of the stacking fault (magnification: 8×10^4) for the specimen of a Ni-Fe–based alloy with oxygen.

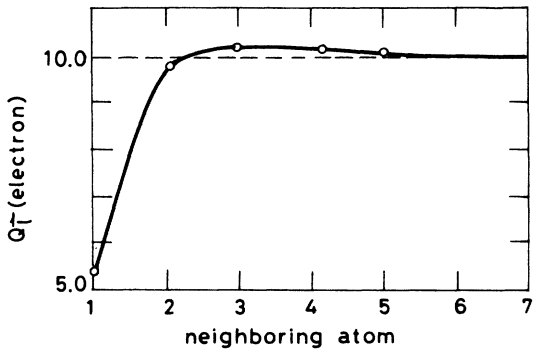

FIG. 14. Variation of valence-electron occupancy with a neighboring atom for the model system with an impurity (oxygen)–stacking-fault complex (the number of valence electrons in an isolated Ni atom is 10).

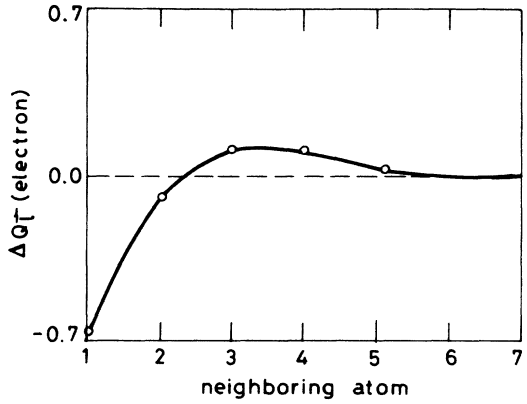

FIG. 15. Transfer of the electron charge of a Ni system with an impurity (oxygen)–stacking-fault complex ($\Delta Q_l=0$ means that the charge transfer is zero).

where Q_l^v, is the total number of valence electrons at site l and $Q_{\alpha l}^v$ is the number of valence electrons of the α orbital at site l.

The electron occupancy of the impurity and its various neighbors is shown in Fig. 14. Corresponding charge-transfer values are shown in Table I and Fig. 15, respectively. Results show that the central oxygen and its first-neighbor Ni lose their electrons, whereas oxygen's second and third neighbors gain some electrons. The charge of oxygen's fourth-neighboring Ni is approximately neutral, which means that there is a heterogeneous region of charge around impurity oxygen. Redistribution of charge is a feature of interaction among the impurity and the host atoms.

The partial-wave integral local density of states is shown in Table II, and gives the information on orbital hybridization. Thus, we can conclude that because of redistribution of charge in a local region of the impurity (oxygen)–stacking-fault complex, partial-wave orbitals of the atom are different from those of a free atom, which is a kind of hybridized local orbital.

V. IMPURITY (OXYGEN)–STACKING-FAULT COMPLEX AND THE MOTION OF DISLOCATION

Based on interest in quantum effects of an impurity-defect complex in a solid, the electronic structure of the complex and the motion of dislocation have been calculated in this paper. The equilibrium equation of various forces acting on a line of dislocation is as follows:

$$\frac{\mu \mathbf{b}_1\cdot\mathbf{b}_2}{2\pi R}+T\frac{d^2r}{dS^2}-E_{\mathrm{SF}}=0\ . \tag{24}$$

In Eq. (24), the first term is the elastic interaction force between two parallel dislocations; R is the distance between two dislocations. The second term is the force acting on the bending dislocation, T is the line tension, $d^2r/dS^2=(R_c)^{-1}$, where R_c is the radius of curvature of the line of the dislocation, and E_{SF} is the stacking-fault energy.

Considering the mixed-type partial dislocation and the feature of constriction, Eq. (24) can be expressed as

$$C\frac{\mu \mathbf{b}_1\cdot\mathbf{b}_2}{2\pi R}+CT\frac{d^2r}{dS^2}-C\frac{\mu \mathbf{b}_1\cdot\mathbf{b}_2}{2\pi D}=0\ , \tag{25}$$

where

$$C=\cos(\psi+\pi/6)\cos(\psi-\pi/6)+\sin(\psi+\pi/6)\sin(\psi-\pi/6)/(1-\nu)\ .$$

C depends on the type of dislocation, and D is the equilibrium width of the extended dislocation.

Based on the feature of the radius of curvature of the line of the dislocation far from the constriction center, $d^2\gamma/dS^2=0$. For this reason, the greater part of the line of the dislocation for the extended dislocation has $E_{\mathrm{SF}}=C\mu\mathbf{b}_1\cdot\mathbf{b}_2/2\pi D$. From it, we can obtain Eq. (25).

In order to obtain a well-organized expression for the constriction energy we refer to Stroh's method;[13] by transforming the equilibrium equation and integrating it, we can obtain

$$E_c=E_1+E_2+E_3=2\left[\frac{\mu \mathbf{b}_1\cdot\mathbf{b}_2}{2\pi}T\right]^{1/2}DI(C)\ , \tag{26}$$

where

$$I(C)=\int_0^1[-C^2\ln(1-v)-C^2v]^{1/2}dv=0.535\,73C\ . \tag{27}$$

TABLE I. Distribution and transfer of electron charge in the model system containing an impurity (oxygen)–stacking-fault complex (units are in electrons).

Neighboring atom	Q_l (valence-electron occupancy at site l)	Q_l (charge transfer at site l)
1	5.3390	−0.6610
2	9.9078	−0.0922
3	10.1132	+0.1132
4	10.1076	+0.1076
5	10.0461	+0.0461

TABLE II. Valence-electron orbital occupancy units are in electrons. For the impurity (1), Q^1–Q^4 correspond to $2S$, $2P_x$, $2P_y$, and $2P_z$ atomic orbitals, and for the neighboring atoms (2–5), Q^1–Q^6 corresponds to $4s$ and $3d_1$–$3d_5$ atomic orbitals.

Neighboring atom	Q^1	Q^2	Q^3	Q^4	Q^5	Q^6
1	1.7404	1.2009	1.2011	1.1967		
2	0.5047	1.8889	1.9195	1.8529	1.9235	1.9269
3	0.4266	1.9615	1.9715	1.9717	1.9605	1.9507
4	0.4270	1.9609	1.9677	1.9740	1.9580	1.9466
5	0.4299	1.9583	1.9001	1.9696	1.9580	1.9556

In Eq. (26), E_1 is the energy corresponding to the repulsive force between dislocations, E_2 is the energy caused by the line tension on the line of the dislocation, E_3 is the surface energy, and $I(C)$ is the parameter introduced by integrating the equilibrium equation, which depends on the type of the dislocation. V is a nondimensional variable introduced by transforming the equilibrium equation.

A jog is a bending segment on the line of the dislocation, whose length is about the distance between the atoms. It can be produced by two dislocations moving on a cross-slip plane.[14]

From Eqs. (15) and (26) it can be seen that the attached surface energy on the stacking-fault plane is related to the constriction energy.

Because jog segment l is very small, the jog energy[13] is as follows:

$$E_j = E_c + \Delta l \varepsilon_e + \Delta l \varepsilon_{\text{mis}} = E_c \ . \tag{28}$$

In Eq. (28), ε_e is the elastic energy of a jog segment, ε_{mis} the misfit energy, and Δl the length of the jog segment.

The corresponding velocity of the climbing of the dislocation[15] is as follows:

$$V_c = bC_jP_j = b \exp\left[-\frac{E_j}{kT}\right] \nu_0 \exp\left[-\frac{\varepsilon_f + \varepsilon_a - Fb^2}{kT}\right] , \tag{29}$$

where F is the motive force of the climbing of the dislocation, b is the length of the Burgers vector, C_j is the concentration of a jog, P_j is the transition probability of a jog, ε_f is formation energy of a vacancy, ε_a is the activation energy of the point defect, F is the elastic force of the climbing of the dislocation, and ν_0 is the atomic vibration frequency. From Eq. (29) it is clear that the attached surface energy on the stacking-fault plane is closely related to the velocity of the climbing of the dislocation, which is related to polygonization and diffusion of vacancies, and affects a series of physical properties of alloys.[1]

The relationship among the velocity of the motion of the dislocation, temperature, and parameter ψ (the angle between the Burgers vector of a perfect dislocation and the line of the dislocation) is shown in Fig. 16. Figure 16 shows that the velocity of the climbing of the approximate screw dislocation (for ψ approaching 0) is conspicuously larger than that of the edge dislocation. On the

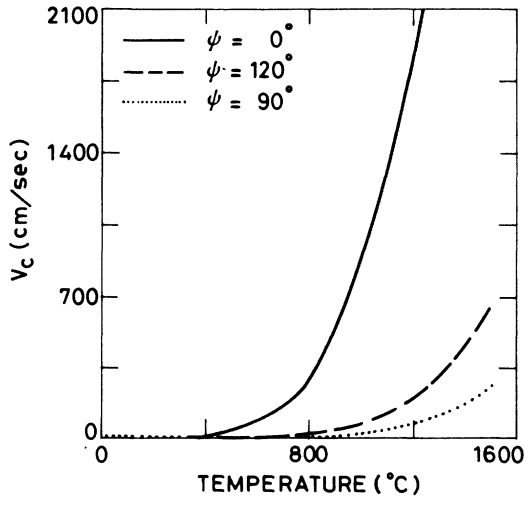

FIG. 16. The relationship among the velocity of the motion of the dislocation, temperature, and parameter ψ (the angle between Burgers vector of perfect dislocation and the line of the dislocation) in a Ni system with an impurity (oxygen)–stacking-fault complex.

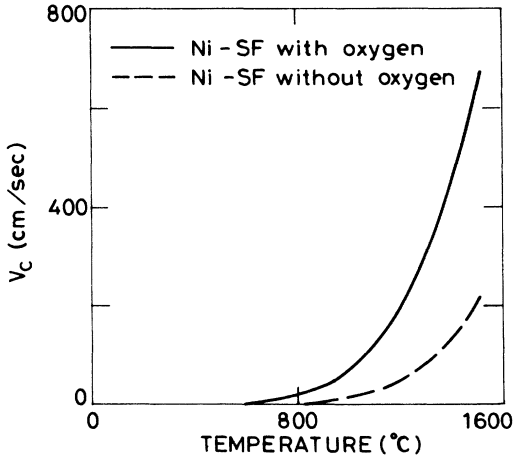

FIG. 17. The relationship between the velocity of the motion of the dislocation and temperature at $\psi = 120°$ for systems with and without oxygen.

basis of the relation between ψ and the width of the extended dislocation, it may be predicted that in the same specimen there are some stacking faults which have different widths corresponding to various kinds of dislocations. The velocities of the motion of the dislocation of systems with and without oxygen are shown in Fig. 17. Results show that the impurity oxygen accelerates the motion of the dislocation.

VI. CONCLUSIONS

(1) The stacking-fault defect lowers the symmetry of d electrons. The charge redistribution of an impurity (oxygen)–stacking-fault complex expresses the feature of the orbital interaction among the impurity oxygen and the host atoms. The calculation of the partial-wave local density of states gives information about local hybridized orbitals.

(2) On the basis of the definition in the paper, by the recursion method, the stacking-fault energy $E_{SF}^{Ni}=152$ erg/cm^2 was given, which approaches the experimental value. Referring to the calculation result for the phonon excitation, and considering the limitation of the classical theory based on the atom bond model, the electron effect is obviously the main contribution to stacking-fault energy.

(3) The attached surface energy of light impurity oxygen on the stacking-fault plane makes the stacking-fault energy of the Ni system increase, whereas the substitutent impurity Fe on the stacking-fault plane makes it decrease markedly. Our related physical idea and calculation results are consistent with the electron-microscope experiment on Ni and Ni-Fe–based alloys.

ACKNOWLEDGMENTS

This work was supported by the National Science Fund. The authors are grateful to Professor Liu Fu-sui and Professor Gu Bin-lin for beneficial discussions.

[1]Tsung-yu Wang *et al.*, IEEE Trans. Magn. **MAG-15**, 1610 (1979).
[2]J. P. Hirth and X. Lothe, *Theory of Dislocations* (Academic, New York, 1968).
[3]Zheng Zhaobo, Shao Zhian, and Wang Chongyu, J. Phys. F **18**, 1137 (1988).
[4]V. Heine, in *Solid State Physics*, edited by H. Ehrenreich, F. Seitz, and D. Turnbull (Academic, New York, 1980), Vol. 35.
[5]R. Haydock, in Ref. 4, p. 216.
[6]J. C. Slater and G. F. Koster, Phys. Rev. **94**, 1498 (1954).
[7]W. A. Harrison, *Electronic Structure and the Properties of Solids* (Freeman, San Francisco, 1980).
[8]C. M. M. Nex, J. Phys. A **11**, 653 (1978).
[9]G. Thomas *et al.*, *Transmission Electron Microscopy of Materials* (Wiley, New York, 1979).
[10]P. B. Hirsch *et al.*, Philos. Trans. R. Soc. London, Ser. A **252**, 499 (1960).
[11]H. Hashimoto *et al.*, Proc. R. Soc. London, Ser. A **269**, 80 (1962).
[12]P. B. Hirsch *et al.*, *Electron Microscope of Thin Crystals* (Butterworths, London, 1971).
[13]A. R. Stroh, Proc. Phys. Soc. London, Sect. B **67**, 427 (1954).
[14]J. Friedel, *Dislocations* (Pergamon, New York, 1964).
[15]A. H. Cottrell, *Dislocations and Plastic Flow in Crystals* (Clarendon, Oxford, 1953).

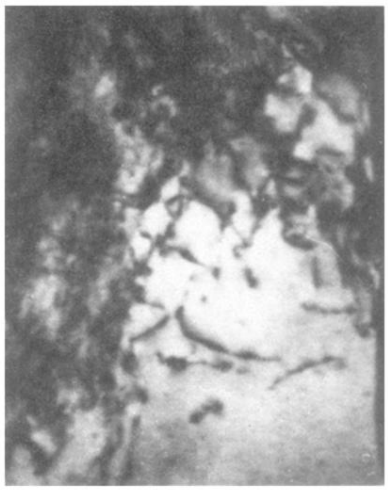

FIG. 10. Electron-microscope image (magnification: 1.35×10^5) for the specimen of the Ni alloy with oxygen.

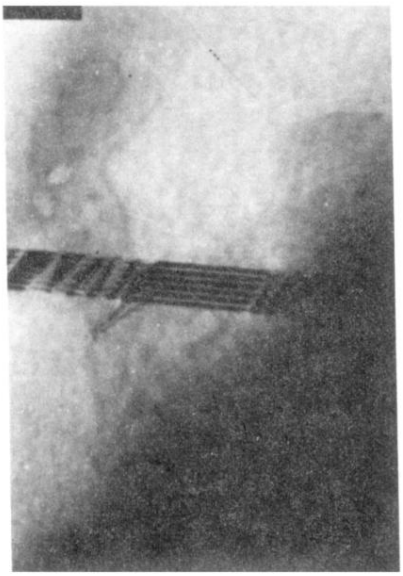

FIG. 11. The image of the stacking fault (magnification: 4.8×10^4) for the specimen of a Ni-Fe–based alloy without oxygen.

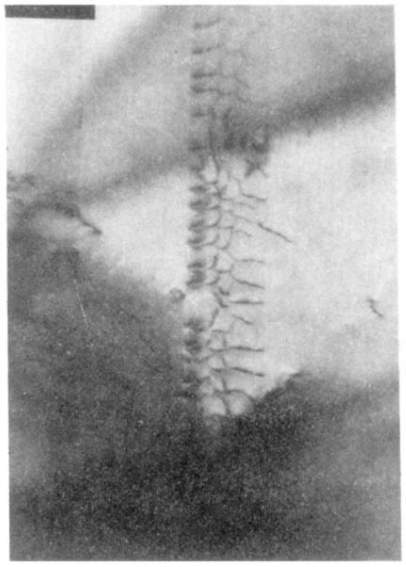

FIG. 12. The typical diffraction contrast image (magnification: 2.8×10^4) for the specimen of a Ni-Fe–based alloy with oxygen.

FIG. 13. The image of the stacking fault (magnification: 8×10^4) for the specimen of a Ni-Fe–based alloy with oxygen.

FIG. 9. The image of an electron microscope (magnification: 1.35×10^5) for the specimen of a Ni alloy without oxygen.